Nanocrystal $[Ti_{14}C_{13}]$ to Metallocarbohedrene $[Ti_8C_{13}]$: Structural Principles and Mechanism

Ian Dance

Contribution from the School of Chemistry, University of New South Wales, Sydney, NSW 2052, Australia

Received August 22, 1995[⊗]

Abstract: Gradient-corrected density functional calculations have characterized the geometric and electronic structures of the metal-carbon clusters $[Ti_{14}C_{13}]^{0,+}$ and $[Ti_8C_{13}]^{0,+}$ and the intermediates Ti_xC_{13} in the sequence of photoextrusions of Ti atoms from $[Ti_{14}C_{13}]^+$ to $[Ti_8C_{13}]^+$. $Ti_{14}C_{13}$ is a vertex-contracted "nanocrystal" fragment of the face-centered cubic TiC lattice, with low-lying spin states, while Ti_8C_{13} is a C^c-centered tetra-Ti^o-capped Ti^i_4 tetrahedron with C_2 groups cradled in six $Ti^i_2Ti^o_2$ butterflies and has a large HOMO-LUMO gap. This sequence of six photodissociations of Ti atoms is significant because it involves the transformation of a fragment of a non-molecular lattice structure to a molecular cluster structure and the formation of six C−C bonds on the surface. The transformation is most endergonic in the first stage to $[Ti_{13}C_{13}]^+$, and decreasingly endergonic to $[Ti_{12}C_{13}]^+$ and $[Ti_{11}C_{13}]^+$. The geometry changes are concerted, with each intermediate partly prepared for the next extrusion of Ti, and the central C^c atom plays a significant role in the substantial structural rearrangements. The high symmetry (O_h) of $[Ti_{14}C_{13}]^+$ is completely lost at $[Ti_{12}C_{13}]^+$, but there is recovery of C_{3v} symmetry at the intermediate $[Ti_{11}C_{13}]^+$ which already has in place the four C^c−Ti^i bonds and the $Ti^i(C_2)_3(Ti^o)_3$ face characteristic of $[Ti_8C_{13}]^+$. Energy changes follow the geometry changes.

Introduction

The range of new binary molecules containing only metal and carbon has expanded dramatically in the last few years.[1] There are at least eight subclasses of new binary metal−carbon compounds: (a) exohedral metallofullerenes;[2−5] (b) endohedral metallofullerenes;[6−12] (c) networked metallofullerenes in which the metal atom(s) is considered to be bonded within the network of carbon atoms at the surface of the fullerene;[13] (d) metallocarbohedrenes, characterized by polyhedral frameworks;[14−16] (e) metal carbide nanocrystallites which are generally conceived as molecular fragments of non-molecular metal carbide lattices;[1c,17,18] (f) relatively flat metal−graphite sheets;[19] (g)

[⊗] Abstract published in *Advance ACS Abstracts,* February 15, 1996.

(1) Reviews (a) Castleman, A. W. *Z. Phys. D* **1993**, *D26*, 159−161. (b) Bowers, M. T. *Acc. Chem. Res.* **1994**, *27*, 324−332. (c) Pilgrim, J. S.; Duncan, M. A. *Adv. Metal Semiconductor Clusters*, **1995**, in press.

(2) (a) Fagan, P. J.; Calabrese, J. C.; Malone, B. *Science* **1991**, *252*, 1160−1161. (b) Fagan, P. J.; Calabrese, J. C.; Malone, B. *J. Am. Chem. Soc.* **1991**, *113*, 9408−9409. (c) Fagan, P. J.; Calabrese, J. C.; Malone, B. *Acc. Chem. Res.* **1992**, *25*, 134−142.

(3) (a) Balch, A. L.; Catalano, V. J.; Lee, J. W. *Inorg. Chem.* **1991**, *30*, 3980−3981. (b) Balch, A. L.; Catalano, V. J.; Lee, J. W.; Olmstead, M. M.; Parkin, S. R. *J. Am. Chem. Soc.* **1991**, *113*, 8953−8955. (c) Balch, A. L.; Catalano, V. J.; Lee, J. W.; Olmstead, M. M. *J. Am. Chem. Soc.* **1992**, *114*, 5455−5457. (d) Balch, A. L.; Lee, J. W.; Olmstead, M. M. *Angew. Chem., Int. Ed. Engl.* **1992**, *31*, 1356−1358. (e) Balch, A. L.; Lee, J. W.; Noll, B. C.; Olmstead, M. M. *Inorg. Chem.* **1994**, *33*, 5238−43.

(4) (a) FeC_{60}: Roth, L. M.; Huang, Y.; Schwedler, J. T.; Cassady, C. J.; Ben-Amotz, D.; Kahr, B.; Freiser, B. S. *J. Am. Chem. Soc.* **1991**, *113*, 6298−6299. (b) $Ni(C_{60})_2$: Huang, Y.; Freiser, B. S. *J. Am. Chem. Soc.* **1991**, *113*, 8186−8187. (c) Kan, S. Z.; Byun, Y. G.; Freiser, B. S. *J. Am. Chem. Soc.* **1995**, *117*, 1177−8.

(5) Douthwaite, R. E.; Green, M. L. H.; Stephens, A. H. H.; Turner, J. F. C. *J. Chem. Soc., Chem. Commun.* **1993**, 1522−1523

(6) Chai, Y.; Guo, T.; Jin, C.; Haufler, R. E.; Chibante, L. P. F.; Fure, J.; Wang, L.; Alford, J. M.; Smalley, R. E. *J. Phys. Chem.* **1991**, *95*, 7564−8.

(7) (a) Yeretzian, C.; Hansen, K.; Alvarez, M. M.; Min, K. S.; Gillan, E. G.; Holczer, K.; Kaner, R. B.; Whetten, R. L. *Chem. Phys. Lett.* **1992**, *196*, 337−342. (b) Gillan, E. G.; Yeretzian, C.; Min, K. S.; Alvarez, M. M.; Whetten, R. L.; Kaner, R. B. *J. Phys. Chem.* **1992**, *96*, 6869−6871.

(8) (a) Yannoni, C. S.; Hoinkis, M.; de Vries, M. S.; Bethune, D. S.; Salem, J. R.; Crowder, M. S.; Johnson, R. D. *Science* **1992**, *256*, 1191−1192. (b) Bethune, D. S.; Johnson, R. D.; Salem, J. R.; de Vries, M.; Yannoni, C. S. *Nature* **1993**, *366*, 123−8.

(9) (a) Rose, H. R.; Dance, I. G.; Fisher, K. J.; Smith, D. R.; Willett, G. D.; Wilson, M. A. *J. Chem. Soc., Chem. Commun.* **1993**, 941−942. (b) Rose, H. R.; Dance, I. G.; Smith, D. R.; Willett, G. D.; Wilson, M. A. *J. Chem. Soc., Chem. Commun.* **1993**, 1361−2.

(10) (a) Kikuchi, K.; Suzuki, S.; Nakao, Y.; Nakahara, N.; Wakabayashi, T.; Shiromaru, H.; Saito, K.; Ikemoto, I.; Achiba, Y. *Chem. Phys. Lett.* **1993**, *216*, 67−68. (b) Kikuchi, K.; Nakao, Y.; Suzuki, S.; Achiba, Y. *J. Am. Chem. Soc.* **1994**, *116*, 9367−68. (c) Kikuchi, K.; Kobayashi, K.; Sueki, K.; Suzuki, S.; Nakahara, H.; Achiba, Y. *J. Am. Chem. Soc.* **1994**, *116*, 9775−6.

(11) (a) Shinohara, H.; Sato, H.; Saito, Y.; Ohkohchi, M.; Ando, Y. *J. Phys. Chem.* **1992**, *96*, 3571−3573. (b) Shinohara, H.; Yamaguchi, H.; Hayashi, N.; Sato, H.; Ohkohchi, M.; Ando, Y.; Saito, Y. *J. Phys. Chem.* **1993**, *97*, 4259−4261. (c) Bandow, S.; Shinohara, H.; Saito, Y.; Ohkohchi, M.; Ando, Y. *J. Phys. Chem.* **1993**, *97*, 6101−6103.

(12) Clemmer, D. E.; Shelimov, K. B.; Jarrold, M. F. *Nature* **1994**, *367*, 718−720.

(13) (a) Clemmer, D. E.; Hunter, J. M.; Shelimov, K. B.; Jarrold, M. F. *Nature* **1994**, *372*, 248−250. (b) Shelimov, K. B.; Jarrold, M. F. *J. Am. Chem. Soc.* **1995**, *117*, 6404−6405.

(14) (a) Guo, B. C.; Kerns, K. P.; Castleman, A. W. *Science* **1992**, *255*, 1411−1413. (b) Guo, B. C.; Wei, S.; Purnell, J.; Buzza, S.; Castleman, A. W. *Science* **1992**, *256*, 515−516. (c) Wei, S.; Guo, B. C.; Purnell, J.; Buzza, S.; Castleman, A. W. *Science* **1992**, *256*, 818−820. (d) Wei, S.; Guo, B. C.; Purnell, J.; Buzza, S.; Castleman, A. W. *J. Phys. Chem.* **1992**, *96*, 4166−4168. (e) Yamada, Y.; Castleman, A. W., Jr. *Chem. Phys. Lett.* **1993**, *204*, 133−138. (f) Cartier, S. F.; May, B. D.; Castleman, A. W. *J. Chem. Phys.* **1994**, *100*, 5384−6. (g) Cartier, S. F.; May, B. D.; Toleno, B. J.; Purnell, J.; Wei, S.; Castleman, A. W. *Chem. Phys. Lett.* **1994**, *220*, 23−28. (h) Cartier, S. F.; May, B. D.; Castleman, A. W. *J. Am. Chem. Soc.* **1994**, *116*, 5295−5297.

(15) (a) Pilgrim, J. S.; Duncan, M. A. *J. Am. Chem. Soc.* **1993**, *115*, 6958−6961. (b) Pilgrim, J. S.; Duncan, M. A. *J. Am. Chem. Soc.* **1993**, *115*, 4395−4396.

(16) (a) Yeh, C. S.; Afzaal, S.; Lee, S. A.; Byun, G.; Freiser, B. S. *J. Am. Chem. Soc.* **1994**, *116*, 8806−8807. (b) Yeh, C. S.; Byun, Y. G.; Afzaal, S.; Kan, S. Z.; Lee, S.; Freiser, B. S.; Hay, P. J. *J. Am. Chem. Soc.* **1995**, *117*, 4042−8.

(17) (a) Pilgrim, J. S.; Duncan, M. A. *J. Am. Chem. Soc.* **1993**, *115*, 9724−9727. (b) Pilgrim, J. S.; Duncan, M. A. *Int. J. Mass Spectrom. Ion Processes* **1994**, *138*, 283−96. (c) Pilgrim, J. S.; Brock, L. R.; Duncan, M. A. *J. Phys. Chem.* **1995**, *99*, 544−550.

(18) Wei, S., Guo, B. C.; Deng, H. T.; Kerns, K.; Purnell, J.; Buzza, S. A.; Castleman, A. W. *J. Am. Chem. Soc.* **1994**, *116*, 4475−6.

(19) Jarrold, M. F. Private communication

0002-7863/96/1518-2699$12.00/0 © 1996 American Chemical Society

carbon nanotubes containing metal atoms;[20] and (h) carbon nanotubes growing from metal clusters.[21,22]

Like the fullerenes, these metal−carbon molecules have raised innumerable new questions: What are the conditions of formation? Which metals can be incorporated? What are the ranges of composition? Which compositions are particularly stable? What are the more stable geometrical structures? What are the electronic structures? How can the more stable of these molecules be prepared as pure bulk samples? While there exist pure samples of some endohedral metallofullerenes, most of these new metal−carbon molecules are still known only in the gas phase.

There are three main lines of experimental approach to the questions of structure. Collisionally induced dissociation and photodissociation of metal carbon clusters have revealed that in general there is a relatively small number of fragmentation products, which can therefore provide information about the structure of the parent.[15b,17,23] In a second approach, the measurement of the drift times of molecular ions through inert gas has allowed both the identification of structural isomers and good estimates of the shapes and sizes of the various molecular ions by comparison of observed and calculated mobilities.[1b,12,13b,24,25] Thirdly, the reactivities of the metal−carbon cluster ions with other molecules such as dioxygen, water, ammonia, acetonitrile, and benzene have been measured and used to infer the number and arrangement of accessible metal atoms as reaction sites.[16,26] Theoretical investigations have also contributed greatly to the development of this science.[16b,27−41]

The first of the metallocarbohedrenes, Ti_8C_{12}, is believed to possess structure **I**, with symmetry T_d: most, but not all, of the theoretical and experimental investigations favor **I** as the most stable structure. There are now at least 15 isomers proposed and evaluated for this prototypical molecule.[42] The prototypical cluster in the "nanocrystallite" class was $Ti_{14}C_{13}$, reported as its positive ion by Duncan,[17] and proposed to possess the structure **II**. A key difference between **I** and **II** is the occurrence of C_2 groups in **I**, and of individual C atoms in **II**. In this context of two stable but chemically different types of TiC cluster, Pilgrim and Duncan described a significant experiment.[17a] They reported that the photofragmentation of $[Ti_{14}C_{13}]^+$ involved successive extrusions of Ti atoms, with the formation of $[Ti_xC_{13}]^+$, $x = 13$, 12, 11, 10, 9, 8, and 7.[1c,17b] $[Ti_8C_{13}]^+$ was the product formed in greatest abundance, and apparently with extra stability, and was assumed to possess a structure based on C-centered Ti_8C_{12}. The importance of the transformation of $Ti_{14}C_{13}$ to Ti_8C_{13} is that it involves C−C bond formation on the surface of a metal cluster, a process which is significant for a number of other areas of chemistry, and for metal-catalyzed growth of carbon nanostructures. Pilgrim and Duncan[17a] suggested a mechanism for their photodissociative transformation, in which the Ti atoms at the face centers of **II** are successively lost, with concomitant formation of the C−C bonds over these faces. In this mechanism the C atom at the center of $Ti_{14}C_{13}$ is that retained as such in Ti_8C_{13}.

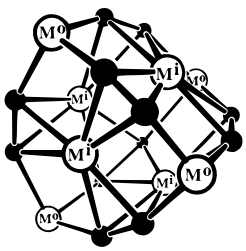

I

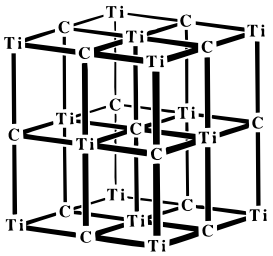

II

In this paper I report the results of density functional modeling of the structures of $Ti_{14}C_{13}$ and Ti_8C_{13}, as uncharged clusters and as the positive ions observed experimentally. In addition, the structures of the intermediates $Ti_{13}C_{13}$, $Ti_{12}C_{13}$, $Ti_{11}C_{13}$, $Ti_{10}C_{13}$, and Ti_9C_{13} are modeled, and the details of the mechanism of transformation of $Ti_{14}C_{13}$ to Ti_8C_{13} are revealed. Nonempirical density functional methods are valuable for such investigations because they include the electron correlation energies, without incurring computational overload. These calculations provide considerable insight into the structures and the structural rearrangements, and the associated energy changes. It becomes apparent that the Ti extrusion processes and the C−C bond formation processes are geometrically concerted.

In related investigations, Reddy and Khanna,[32b,32c] using density functional methods, have optimized structure **II** for $[Ti_{14}C_{13}]^0$ with only one variable, the Ti−C distance. Rohmer, Benard et al.[28c] expected (on the basis of electron population) that the cubic (O_h) structure of $Ti_{14}C_{13}$ would distort to T_d with the eight corner Ti atoms breaking into two subsets and optimized the resulting quintet state with a single configuration

(20) Lago, R. M.; Tsang, S. C.; Lu, K. L.; Chen, Y. K.; Green, M. L. H. *J. Chem. Soc., Chem. Commun.* **1995**, 1355−1356.
(21) Bethune, D. S.; Kiang, C.-H.; de Vries, M. S.; Gorman, G.; Savoy, R.; Vazquez, J.; Beyers, R. *Nature* **1993**, *363*, 605.
(22) Guerret-Plècourt, C.; Le Bouar, Y.; Loiseau, A.; Pascard, H. *Nature* **1994**, *372*, 761−5.
(23) (a) Wei, S.; Guo, B. C.; Purnell, J.; Buzza, S. A.; Castleman, A. W. *J. Phys. Chem.* **1993**, *97*, 9559−9561. (b) Purnell, J.; Wei, S.; Castleman, A. W. *Chem. Phys. Lett.* **1994**, *229*, 105−110.
(24) (a) von Helden, G.; Hsu, M.-T.; Gotts, N.; Bowers, M. T. *J. Phys. Chem.* **1993**, *97*, 8182−8192. (b) von Helden, G.; Gotts, N. G.; Maitre, P.; Bowers, M. T. *Chem. Phys. Lett.* **1994**, *227*, 601−8. (c) Lee, S.; Gotts, N. G.; von Helden, G.; Bowers, M. T. *Science* **1995**, *267*, 999−1001.
(25) (a) Shelimov, K. B.; Clemmer, D. E.; Jarrold, M. F. *J. Phys. Chem.* **1994**, *98*, 12819−21. (b) Shelimov, K. B.; Clemmer, D. E.; Jarrold, M. F. *J. Phys. Chem.* **1995**, *99*, 11376−11386. (c) Clemmer, D. E.; Jarrold, M. F. *J. Am. Chem. Soc.* **1995**, *117*, 8841−8850.
(26) (a) Guo, B. C.; Castleman, A. W., Jr. *J. Am. Chem. Soc.* **1993**, *115*, 7415−8. (b) Deng, H. T.; Guo, B. C.; Kerns, K. P.; Castleman, A. W. *J. Phys. Chem.* **1994**, *98*, 13373−13378. (c) Kerns, K. P.; Guo, B. C.; Deng, H. T.; Castleman, A. W. *J. Am. Chem. Soc.* **1995**, *117*, 4026−9.
(27) (a) Dance, I. G. *J. Chem. Soc., Chem. Commun.* **1992**, 1779−1780. (b) Dance, I. G. *J. Chem. Soc., Chem. Commun.* **1993**, 1306−8. (c) Dance, I. G. *J. Am. Chem. Soc.* **1993**, *115*, 11052−3.
(28) (a) Rohmer, M.-M.; de Vaal, P.; Benard, M. *J. Am. Chem. Soc.* **1992**, *114*, 9696−9697. (b) Rohmer, M.-M.; Benard, M.; Henriet, C.; Bo, C.; Poblet, J.-M. *J. Chem. Soc., Chem. Commun.* **1993**, 1182−1185. (c) Rohmer, M.-M.; Benard, M.; Bo, C.; Poblet, J.-M. *J. Am. Chem. Soc.* **1995**, *117*, 508−517.
(29) Ceulemans, A.; Fowler, P. W. *J. Chem. Soc., Faraday Trans. 1* **1992**, *88*, 2797−2798.
(30) (a) Zhenyang, L.; Hall, M. B. *J. Am. Chem. Soc.* **1992**, *114*, 10054−5. (b) Lin, Z.; Hall, M. B. *J. Am. Chem. Soc.* **1993**, *115*, 11165−11168.
(31) (a) Grimes, R. W.; Gale, J. D. *J. Chem. Soc., Chem. Commun.* **1992**, 1222−1224. (b) Grimes, R. W.; Gale, J. D. *J. Phys. Chem.* **1993**, *97*, 4616−4620.
(32) (a) Reddy, B. V.; Khanna, S. N.; Jena, P. *Science* **1992**, *258*, 1640−1643. (b) Reddy, B. V.; Khanna, S. N. *Chem. Phys. Lett.* **1993**, *209*, 104−108. (c) Reddy, B. V.; Khanna, S. N. *J. Phys. Chem.* **1994**, *98*, 9446−49.
(33) Hay, P. J. *J. Phys. Chem.* **1993**, *97*, 3081−3083.
(34) Methfessel, M.; Schilfgaarde, M. van; Scheffler, M. *Phys. Rev. Lett.* **1993**, *70*, 29−32.
(35) Guo, T.; Odom, G. K.; Scuseria, G. E. *J. Phys. Chem.* **1994**, *98*, 7745−47.
(36) Pauling, L. *Proc. Natl. Acad. Sci. U.S.A.* **1992**, *89*, 8175−8176.
(37) Chen, H.; Feyereisen, M.; Long, X. P.; Fitzgerald, G. *Phys. Rev. Lett.* **1993**, *71*, 1732−5.
(38) (a) Lou, L.; Guo, T.; Nordlander, P.; Smalley, R. E. *J. Chem. Phys.* **1993**, *99*, 5301−5305. (b) Lou, L.; Nordlander, P. *Chem. Phys. Lett.* **1994**, *224*, 439−444.
(39) Nagase, S.; Kobayashi, K. *J. Chem. Soc., Chem. Commun.* **1994**, 1837−1838.
(40) Jackson, K.; Kaxiras, E.; Pederson, M. R. *J. Phys. Chem.* **1994**, *98*, 7805−7810.
(41) Li, Y. S.; Tomanek, D. *Chem. Phys. Lett.* **1994**, *221*, 453−8.
(42) Dance, I. G. In preparation, 1995.

HF calculation. Lou and Nordlander[38b] applied local density functional methods to the structure of Ti_8C_{13} and concluded that the most stable geometry is that with a tetrahedral four-coordinate C atom at the center of the T_d structure of Ti_8C_{12}. In relevant experimental work, Bowers et al.[1b,24c] measured the mobility of $[Ti_8C_{13}]^+$ (generated directly and not by photodissociation of $[Ti_{14}C_{13}]^+$) in helium and detected only one isomer which was modeled best as Ti_8C_{12} with one exohedral carbon atom bound to Ti.

Methodology

The electronic structures and energies are computed using density functional (DF) methods, with geometry optimization by minimization of the energy gradients. The inclusion of electron correlation and electron exchange energies in DF calculations, while maintaining computational expediency, permits reliable calculations on large metal clusters. The computational expediency is not at the expense of accuracy, as has been demonstrated in many investigations of transition metal complexes and inorganic clusters. The original DF methods used local density functionals (LDF), which overestimate binding energies and shorten bond distances, but the incorporation of gradient corrections in nonlocal density functionals (NLDF) returns acceptable energies and geometries.[43−52] In separate publications I report extensive investigations of the reliability of LDF and NLDF methods for calculation of the known geometries of metal−chalcogenide clusters and evaluation of LDF and NLDF calculations of the multiple isomers of Ti_8C_{12}, in comparison with more conventional SCF/CI calculations.[53] In general the calculated bond distances involving metal and other high-Z atoms are accurate to ca. 0.05 Å, and indeed the accuracy improves as the size of the cluster increases. Therefore, for large inorganic molecules such as metal−carbon clusters, NLDF computations provide an effective and expedient methodology for exploration and description of geometry−energy hypersurfaces.

The computations reported here used the program DMol.[50,54,55] Double numerical basis sets with polarization functions were used; core orbitals were frozen.[56,57] The LDF calculations reported below employed the Hedin−Lunqvist representation of the exchange-correlation energy of a homogeneous electron gas.[58] Two NLDF functionals were used: (i) vwn/b88 employs the Vosko−Wilke−Nusair[59] functional for the local electron correlation, the Hartree−Fock−Slater $\rho^{1/3}$ local exchange function, and the Becke[60] nonlocal correction for exchange; (ii) lyp/b88 uses instead the Lee−Yang−Parr functional[61] for the local and nonlocal components of correlation. For each structure independent optimizations were undertaken for the different functionals. In most cases the nonlocal corrections were applied to the energy after the SCF calculation: calculations using these post-SCF corrections are labeled vwn/b88e or lyp/b88e in the following. Although this method is expected to be less accurate than application of the nonlocal corrections to the potential during convergence of the SCF calculation, experience[53] shows that the reduction in accuracy is small and is outweighed by the gain in computational efficiency when exploring the energy surfaces of large clusters. Spin-unrestricted calculations were used for the positive ions with an odd number of electrons, and both spin-restricted and spin-unrestricted calculations were used for the even-electron neutral clusters. Calculational meshes for the electron density were medium or fine grade: the improvement in precision for the fine mesh is generally marginal for evaluation of clusters as in this paper. During the geometry optimizations by gradient methods the molecules were constrained to symmetries generally lower than the highest possible. Some smearing of electron density over molecular orbitals at the Fermi level was incorporated in the initial stages of calculations: for large clusters this has the advantageous effect of averaging the structure over any low-lying excited states. Atom partial charges were calculated by the Mulliken method, and ionization energies were calculated from the binding energy of the cation at the optimized geometry for the neutral cluster.

Table 1 is a catalog of the calculations and provides the calculated binding energies. Atomic coordinates and geometrical properties of all optimized structures are included in the supporting information. These data can be used to calculate ion mobilities for comparison with ion drift measurements.

Table 1. Optimization Calculations and Binding Energies for Optimized Structures

structure	charge	symmetry of opt	calculation	binding energy: total, kcal mol^{-1}	binding energy: per atom, kcal mol^{-1} [eV]
			Non-Local Density Functionals		
Ti_8C_{13}-T_d	0	D_2	vwn/b88e	−2849.4	−135.7 [−5.88]
	0	D_2	lyp/b88e	−2980.0	−141.9 [−6.15]
	+	D_2	vwn/b88e	−2717.5	−129.4 [−5.61]
	+	D_2	lyp/b88e	−2856.5	−136.0 [−5.90]
$Ti_{11}C_{13}$	0	C_1	lyp/b88e	−3328.9	−138.7 [−6.01]
	+	C_1	vwn/b88e	−3034.7	−126.4 [−5.48]
$Ti_{12}C_{13}$	0	C_1	lyp/b88e	−3346.8	−133.9 [−5.81]
	+	C_1	vwn/b88e	−3048.8	−122.0 [−5.29]
$T_{13}C_{13}$	0	C_{2v}	vwn/b88e	−3283.0	−126.3 [−5.48]
	+	C_{2v}	vwn/b88e	−3170.9	−122.0 [−5.29]
	0	C_2	vwn/b88e	−3305.8	−127.1 [−5.51]
	0	C_2	lyp/b88e	−3467.8	−133.4 [−5.78]
	+	C_2	vwn/b88e	−3190.5	−122.7 [−5.32]
$Ti_{14}C_{13}$	0	D_2	vwn/b88e	−3547.4	−131.4 [−5.70]
	0	D_2	lyp/b88e	−3716.0	−137.6 [−5.97]
	+	D_2	vwn/b88e	−3448.8	−127.7 [−5.54]
	+	D_2	lyp/b88e	−3618.2	−134.0 [−5.81]
			Local Density Functionals		
Ti_8C_{13}-T_d	0	D_2	LDF	−3581	−170.5 [−7.39]
$Ti_{11}C_{13}$	0	C_1	LDF	−3894	−162.3 [−7.04]
$Ti_{12}C_{13}$	0	C_1	LDF	−4037	−161.5 [−7.00]
$Ti_{13}C_{13}$	0	C_{2v}	LDF	−4199	−161.5 [−7.00]
$Ti_{14}C_{13}$	0	D_2	LDF	−4532	−167.9 [−7.28]

Results

The geometric and electronic structures for the two main clusters $[Ti_{14}C_{13}]^{0,+}$ and $[Ti_8C_{13}]^{0,+}$ are presented first, followed by the structures and properties of the intermediates, and finally the energy changes during the reaction sequence. Structures for $[Ti_xC_y]$ are labeled x/y: Ti^i and Ti^o refer to inner and outer Ti atoms in Ti_8C_{12} and Ti_8C_{13}, and C^c denotes the central C

(43) (a) Ziegler, T.; Tschinke, V.; Versluis, L.; Baerends, E. J.; Ravenek, W. *Polyhedron* **1988**, *7*, 1625−1637. (b) Folga, E.; Ziegler, T. *J. Am. Chem. Soc.* **1993**, *115*, 5169−76. (c) Jacobsen, H.; Schreckenbach, G.; Ziegler, T. *J. Phys. Chem.* **1994**, *98*, 11406−10.

(44) Pacchioni, G.; Rösch, N. *Inorg. Chem.* **1990**, *29*, 2901−08.

(45) Peluso, A.; Salahub, D. R.; Goursot, A. *Inorg. Chem.* **1990**, *29*, 1544−49.

(46) (a) Rosa, A.; Baerends, E. J. *Inorg. Chem.* **1992**, *31*, 4717−26. (b) Leeuwen, R. Van; Baerends, E. J. *Int. J. Quantum Chem.* **1994**, *52*, 711.

(47) (a) Sosa, C.; Andzelm, J. W.; Elkin, B. C.; Wimmer, E.; Dobbs, K. D.; Dixon, D. A. *J. Phys. Chem.* **1992**, *96*, 6630−6636. (b) Dixon, D. A.; Gole, J. L. *Chem. Phys. Lett.* **1992**, *189*, 390−394.

(48) Andzelm, J.; Sosa, C.; Eades, R. A. *J. Phys. Chem.* **1993**, *97*, 4664−9.

(49) (a) Deeth, R. J. *J. Chem. Soc., Faraday Trans.* **1993**, *89*, 3745−9. (b) Deeth, R. J.; Field, C. N. *J. Chem. Soc., Dalton Trans.* **1994**, 1943−1948.

(50) Delley, B.; Wrinn, M.; Lüthi, H. P. *J. Chem. Phys.* **1994**, *100*, 5785−91.

(51) Russo, T. V.; Martin, R. L.; Hay, P. J. *J. Chem. Phys.* **1994**, *101*, 7729−37.

(52) Bohr, F.; Chermette, H.; Ruiz-Lopez, M. F. *Int. J. Quantum Chem.* **1994**, *52*, 1039−49.

(53) Dance, I. G. In preparation.

(54) Biosym Technologies, Inc., San Diego, USA; v2.3 and v2.36.

(55) Delley, B. *J. Chem. Phys.***1990**, *92*, 508−517.

(56) Basis set DND, which for Ti comprises 1s, 2s, 2p, 3s, 3p, 3d, and 4s orbitals computed for Ti^0; with 3d, 4s, and 4p orbitals computed for Ti^{2+}: for C the DND basis set comprises 1s, 2s, and 2p computed for C^0; and 2s, 2p, 3d for C^{2+}. The frozen core configurations were C $1s^2$; Ti $1s^2$, $2s^2$, $2p^6$.

(57) Details of the basis sets and tabulations of all dimensions and atomic coordinates, are included in the supporting information.

(58) Hedin, L.; Lundqvist, B. I. *J. Phys. C* **1971**, *4*, 2064−2083: this is the functional labeled JMW in DMol.

(59) Vosko, S. H.; Wolke, L.; Nusair, M. *Can. J. Phys.***1980**, *58*, 1200−1211.

(60) Becke, A. D. *Phys. Rev. A* **1988**, *38*, 3098.

(61) Lee, C.; Yang, W.; Parr, R. G. *Phys. Rev. B* **1988**, *37*, 785−789.

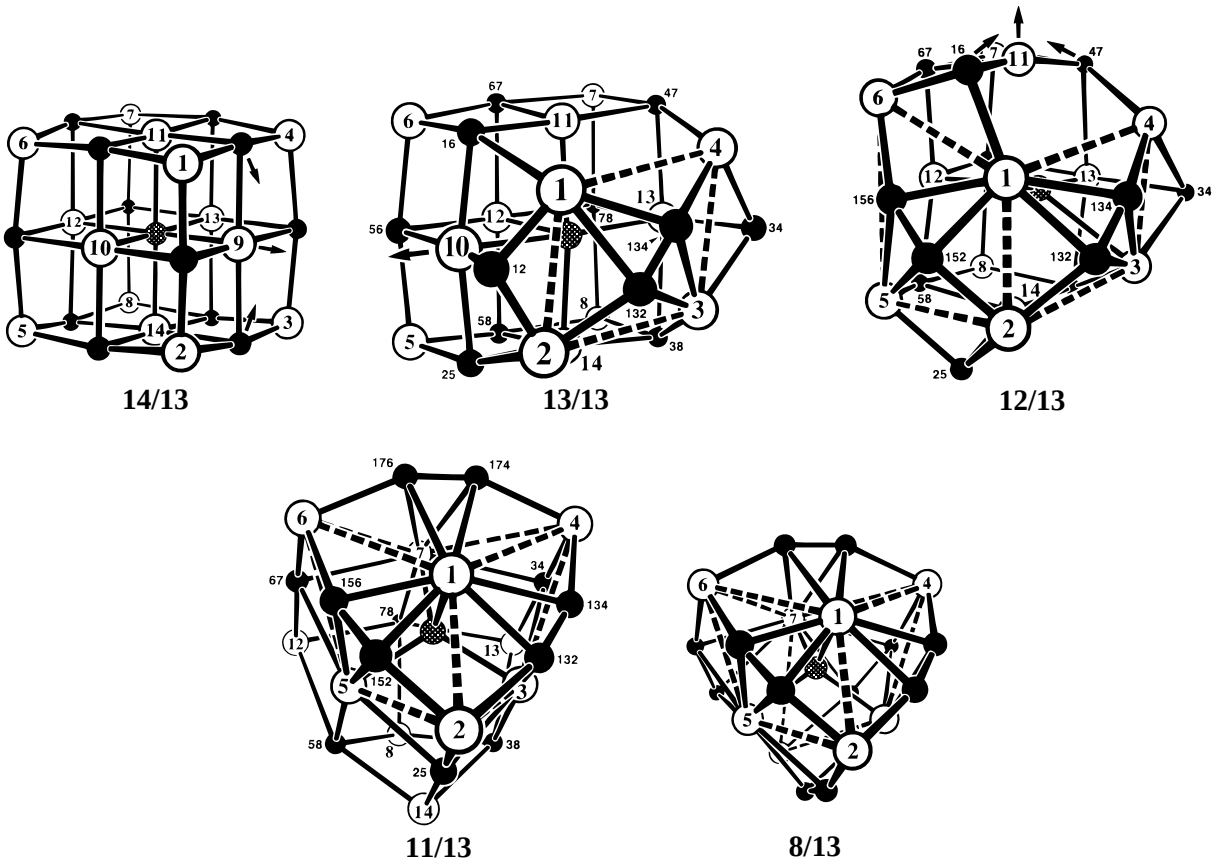

Figure 1. Optimized structures of $[Ti_xC_{13}]$ for $x = 14$, 13, 12, 11, 8, denoted ***x*/13**. The central carbon atom, C^c, is stippled, all other carbon atoms are filled, and the Ti atoms are open circles. Titanium atoms retain the number labels of **14/13** throughout the sequence of structures. Single carbon atoms are labeled C*xy* where *x* and *y* are the lowest numbers for the Ti atoms to which C*xy* is bound; carbon atoms in C_2 groups are labeled C*xyz*, where T*ix* and T*iy* are the side-bound Ti atoms and T*iz* forms the end-bond. New Ti_4 faces formed during extrusion processes are indicated with broken Ti−Ti bonds. The arrows show the movement of atoms in the progression to the next intermediate. The first stage, **14/13**−Ti9 → **13/13**, results in C^c−Ti10 becoming 0.1 Å longer than C^c−Ti11 and C^c−Ti14. During the second stage **13/13**−Ti10 → **12/13**, Ti1 and Ti3 (which both eventually become Ti^i) are drawn toward C^c. The loss of Ti11 in the third stage to form **11/13** causes recovery of 3-fold symmetry (about the Ti8−C^c−Ti1 axis), and the formation of three C_2 groups in wheel formation around Ti1. The four bonds between C^c and Ti1, Ti3, Ti5, and Ti7 (which become the Ti^i in the final product) are already formed, and the eventual Ti^o atoms Ti2, Ti4, and Ti6 are in place. In **8/13** the broken lines mark the Ti^i − Ti^o connections: Ti^i−Ti^i connections are not drawn.

atom. The differentiation of atom types in some structures is achieved with the notation E^n, in which the superscript is the coordination number, that is the number of bonded atoms of the other element.

$Ti_{14}C_{13}$. A completely orthogonal face-centered cubic fragment, **II**, was optimized under symmetry D_2 and underwent small but significant changes to structure **14/13** in Figure 1. The geometry was optimized for both the neutral cluster and the positive ion as observed, but there was no significant difference between them: the largest difference was 0.007 Å in the Ti^5−C^4 distance in the face of the cluster.[62] The cubic fragment **II** changes in the expected fashion, with the lesser coordinated Ti^3 atoms at the vertices drawn inwards slightly. Geometrical details are provided in Table 2. The bonds to the lesser-coordinated Ti^3 atoms are ca. 0.12 Å shorter than the bonds to the Ti^5 atoms, as expected. The most relevant experimental datum for comparison is the Ti^6−C^6 distance in the face-centered cubic structure of TiC, 2.16 Å,[63] which is entirely consistent with the present NLDF values of 2.13 Å for Ti^5−C^6 and 2.18 (2.17) Å for Ti^5−C^4. The LDF optimization by Reddy and Khanna[32c] of the orthogonal structure with Ti−C as the only variable yielded all Ti−C = 2.04 Å, while Benard's HF-SCF optimization without CI yielded Ti^5−C^4 = 2.12 Å and Ti^3−C^4 = 2.03 Å.[28c]

(62) The superscript in the notation E^n is the coordination number, that is the number of bonded atoms of the other element.

(63) *Struct. Rep.* **1955**, *19*, 86−87.

Table 2. Interatomic Distances (Å) in the Structures of $[Ti_{14}C_{13}]$ and $[Ti_{14}C_{13}]^+$, Optimized with Different Functionals[a]

	$[Ti_{14}C_{13}]^0$		$[Ti_{14}C_{13}]^+$		$[Ti_{14}C_{13}]^0$
bond	vwn/b88e	lyp/b88e	vwn/b88e	lyp/b88e	LDF
Ti^5−C^6	2.13	2.12	2.13	2.13	2.06
Ti^5−C^4	2.17	2.18	2.16	2.17	2.10
Ti^3−C^4	2.05	2.05	2.05	2.05	1.99
Ti^5−Ti^5	3.02	3.00	3.02	3.01	2.91
Ti^5−Ti^3	2.89	2.88	2.89	2.89	2.80
C^6- -Ti^3	3.54	3.53	3.54	3.54	3.43

[a] The atom types are $C^6 = C^c$, C^4, Ti^3, Ti^5, and the symmetry is O_h, even though D_2 symmetry only was imposed.

The cluster dimensions are almost invariant with cluster charge, which is not surprising because the partially occupied orbitals are essentially nonbonding. The orbital structures calculated for $[Ti_{14}C_{13}]^0$ and $[Ti_{14}C_{13}]^+$ at their optimized geometries are similar. At the Fermi level of $[Ti_{14}C_{13}]^0$, the lyp/b88e calculation shows a 3-fold degenerate HOMO at −2.68 eV populated by four electrons, with a gap of 0.19 eV to the LUMO, while the unrestricted spin calculation (lyp/b88e) for $[Ti_{14}C_{13}]^+$ yields a degenerate HOMO containing three electrons at −5.87 eV with a gap of 0.20 eV to the LUMO. Spin multiplet states are expected. The partially occupied orbitals are comprised mainly of Ti^3 (3d), with some Ti^5 (3d) and less C^4 (2p). Atom partial charges for $[Ti_{14}C_{13}]^0$ are calculated to be Ti^5 +0.86,Ti^3 +0.73, C^6 −1.05, C^4 −0.83: the corresponding values

Table 3. Interatomic Distances (Å) in the T_d Structures of $[Ti_8Cl_{13}]$, $[Ti_8C_{13}]^+$, $[Ti_8C_{12}]$, and $[Ti_8C_{12}]^+$ [a]

	$[Ti_8C_{13}]^0$			$[Ti_8C_{13}]^+$		$[Ti_8C_{12}]^0$		$[Ti_8C_{12}]^+$	
bond	vwn/b88e	lyp/b88e	*b*	vwn/b88e	lyp/b88e	vwn/b88e	lyp/b88e	vwn/b88e	lyp/b88e
C^c-Ti^i	1.90	1.88		1.93	1.90	–	(1.80[c])	–	–
Ti^i-C	2.32	2.31	2.23	2.30	2.31	2.28	2.27	2.27	2.25
Ti^o-C	2.05	2.04	1.97	2.05	2.04	2.01	2.00	2.01	2.00
C−C	1.34	1.36	1.35	1.35	1.35	1.35	1.35	1.34	1.35
Ti^i-Ti^i	3.10	3.08		3.15	3.10	2.94	2.94	2.93	2.91
Ti^i-Ti^o	3.03	3.02	2.96	3.05	3.02	2.96	2.96	2.98	2.98
Ti^o- -Ti^o	5.02	5.01		5.06	5.01	4.94	4.94	4.98	4.98
C^c- -Ti^o	3.08	3.07		3.10	3.07		(3.02[c])		
C^c- -C	2.77	2.75		2.74	2.75		(2.71[c])		

[a] C^c is the central C atom, Ti^i and Ti^o are the inner and outer Ti atoms, and C belongs to C_2. Symmetry D_2 was imposed. [b] Values reported by Lou and Nordlander.[38b] [c] Distances from the unoccupied centroid of Ti_8C_{12}.

for $[Ti_{14}C_{13}]^+$ are Ti^5 +0.89, Ti^3 +0.81, C^6 −1.04, C^4 −0.82. The ionization energy of $[Ti_{14}C_{13}]^0$ is calculated (lyp/b88e) to be 4.41 eV.

Rohmer, Benard, et al.[28c] expected on the basis of electron population that the cubic (O_h) structure of $Ti_{14}C_{13}$ would distort to T_d, with the eight vertex Ti atoms breaking into two subsets. They optimized the resulting quintet state with a single-configuration HF calculation, obtaining a differentiation of Ti^3-C^4 distances to 1.99 and 2.07 Å, with a concomitant energy stabilization of 13 kcal mol^{-1}. I have investigated this possible symmetry reduction with optimization of $[Ti_{14}C_{13}]^+$, starting at a T_d structure in which the Ti^3-C^4 distances were differentiated by 0.1 Å: on optimization with no symmetry constraints the structure reverted to its original energy minimum in virtual O_h symmetry.

The binding energies (see Table 1) for $[Ti_{14}C_{13}]^0$ and $[Ti_{14}C_{13}]^+$ respectively were 5.70 and 5.54 eV mol^{-1} per atom (vwn/b88e functional) and 5.97 and 5.81 eV mol^{-1} per atom (lyp/b88e functional). Although there is no experimental datum against which to check these calculations, the cohesive energy of 7.1 eV mol^{-1} per atom for non-molecular Ti−C is relevant, as an upper limit.[64] Using LDF, Reddy and Khanna[32b] calculated 6.74 eV mol^{-1} per atom for exactly cubic $[Ti_{14}C_{13}]$.

Ti_8C_{13}. The C-centered T_d structure for Ti_8C_{13}, structure **8/13** in Figure 1, was optimized with symmetry D_2 imposed as both $[Ti_8C_{13}]^0$ and $[Ti_8C_{13}]^+$. The key features of the structure are a central atom C^c, tetrahedrally coordinated to four inner Ti^i atoms, with four outer Ti^o atoms capping the faces of the $(Ti^i)_4$ tetrahedron. The surface is comprised of six equivalent folded $(Ti^i)_2(Ti^o)_2$ rhombuses, each of which binds a C_2 group parallel to its long axis. Each surface unit adopts a conformation described as "$(Ti^i)_2(Ti^o)_2$ canoe plus (C_2) canopy", with the Ti^o atoms at the prow and stern of the canoe. Geometrical details are presented in Table 3 in comparison with the corresponding values for the most stable T_d isomer of $[Ti_8C_{12}]^0$ and $[Ti_8C_{12}]^+$. The presence of a carbon atom at the centroid of the structure of Ti_8C_{12} causes an expansion of the central $(Ti^i)_4$ tetrahedron: the C^c-Ti^i distances in $[Ti_8C_{13}]^{0,+}$ are 0.10−0.13 Å longer than the centroid−Ti^i distances in $[Ti_8C_{12}]^{0,+}$, and the Ti^i-Ti^i distances in Ti_8C_{13} are longer by ca. 0.2 Å than those in Ti_8C_{12}. However, the addition of C^c in Ti_8C_{13} has less effect on the outer regions of the cluster, expanding the Ti^o sphere by 0.05 Å and the C sphere by 0.04 Å. The geometry of the binding of the C_2 groups within the $(Ti^i)_2(Ti^o)_2$ canoe is very slightly expanded in $T_d-Ti_8C_{13}$ compared with $T_d-Ti_8C_{12}$: the C−C bond lengths are the same, 1.35 Å. Removal of one electron from $[Ti_8C_{13}]^0$ expands the structure very slightly.

While the increased connectivity at Ti^i due to the addition of the central carbon atom would normally elongate bonds such as Ti^i-Ti^i, I suggest that the calculated expansion indicates that the $C^c(Ti^i)_4$ core is subject to compressive stress, and that a $T_d-X(M^i)_4(M^o)_4(C_2)_6$ structure with slightly smaller X or slightly larger M would be more stable.

The binding energies calculated for $[Ti_8C_{13}]$ are 6.15 (lyp/b88e) and 5.88 (vwn/b88e) eV mol^{-1} $atom^{-1}$, compared with 6.19 (lyp/b88e) and 5.92 (vwn/b88e) eV mol^{-1} $atom^{-1}$ for $[Ti_8C_{12}]$. For the corresponding positive ions, the binding energies are 5.90 (lyp/b88e) and 5.61 (vwn/b88e) eV mol^{-1} $atom^{-1}$ for $[Ti_8C_{13}]^+$ and 5.95 (lyp/b88e) and 5.69 (vwn/b88e) eV mol^{-1} $atom^{-1}$ for $[Ti_8C_{12}]^+$. The slightly smaller values for Ti_8C_{13} also suggest that the incorporation of the central carbon atom is mildly destabilizing. A similar conclusion was reached also by Lou and Nordlander[38b] using LDF.

The electronic structure for $[Ti_8C_{13}]^0$, calculated at the optimized geometry, comprises a HOMO $(t_2)^6$ at −3.5 eV, with a separation of 1.02 eV to the t_2 LUMO. Lou and Nordlander[38b] calculated the HOMO-LUMO separation for T_d-$[Ti_8C_{13}]^0$ to be 1.17 eV. The atom partial charges for $[Ti_8C_{13}]^0$ ($[Ti_8C_{13}]^+$ values in parentheses) are C^c −0.91 (−0.93), Ti^i +0.80 (+0.84), Ti^o +0.66 (+0.77), C −0.41 (−0.38): the charges for $[Ti_8C_{13}]^0$ agree well with those reported by Lou and Nordlander.[38b] The ionization energy for $[Ti_8C_{13}]^0$ is calculated to be 5.4 eV with the lyp/b88e functional and 5.7 eV with the vwn/b88e functional.

The central cavity within the hexahedral-Ti_8 core of the T_h isomeric structure for Ti_8C_{12} is too large to bind a C atom. By imposition of symmetry D_{2h} this C-centered T_h structure of $[Ti_8C_{13}]^+$ was optimized (vwn/b88e, unrestricted spin) as such, and calculated to be 256 kcal mol^{-1} less stable than the C-centered T_d structure **8/13** optimized in the same way, and therefore was not considered further.

I note in passing that there are other possible isomeric structures for $[Ti_8C_{13}]$, derived from the many other possibilities for $[Ti_8C_{12}]$, by incorporation of a central C atom. Lou and Nordlander[38b] found that the calculated binding energy for one such alternative (D_{2d}) was less favorable than the T_d structure. The only experimental data are from Bowers et al.,[1b,24c] who generated $[Ti_8C_{13}]^+$ by laser vaporization of Ti^+ followed by supersonic expansion in He/CH_4, and subsequently observed only one peak when $[Ti_8C_{13}]^+$ drifted through He under weak electric field. The cross section for $[Ti_8C_{13}]^+$ calculated from the drift velocity was compared with the calculated cross-sections for two structures, **8/13** and the T_h-Ti_8C_{12} framework with a *external* C atom bonded to only one Ti atom. The agreement was better for this latter structure, and thus there is a conflict between the calculations on Ti_8C_{13} and the interpretation of the measured cross section. This raises the question as to whether $[Ti_8C_{13}]^+$ generated in the Bowers experiment is the same as $[Ti_8C_{13}]^+$ generated by dissociation of Ti from

(64) The binding energy calculated for $[Ti_{14}C_{13}]^0$ optimized with the local density functional JMW was 7.28 eV mol^{-1} per atom, and is clearly too large.

Table 4. Selected[a] Dimensions (Å) of the Optimized Structure, **13/13**, of $[Ti_{13}C_{13}]$ and $[Ti_{13}C_{13}]^+$, in Symmetry C_2

bond antecedents in $Ti_{14}C_{13}$	bond[b]	$[Ti_{13}C_{13}]^0$ lyp/b88e	$[Ti_{13}C_{13}]^+$ vwn/b88e
C^6-Ti^5	C^c-Ti11	2.10	2.09
C^6-Ti^5	C^c-Ti10	2.21	2.25
C^6-Ti^5	C^c-Ti12	2.24	2.33
C^6-Ti^3	C^c-Ti1	2.80	2.81
C^6-Ti^3	C^c-Ti2	3.29	3.30
Ti^3-Ti^3	Ti1−Ti4	3.44	3.44
Ti^3-Ti^3	Ti1−Ti2	2.95	2.98
Ti^3-Ti^3	Ti1−Ti3	3.85	3.91
none	C132−C134	1.37	1.36
Ti^3-C^4	Ti1−C134	2.23	2.24
Ti^3-C^4	Ti1−C132	2.27	2.31
Ti^3-C^4	Ti2−C132	2.08	2.10
Ti^3-C^4	Ti1−C12	1.96	1.95
Ti^3-C^4	Ti2−C12	1.92	1.90
Ti^3-C^4	Ti1−C16	2.39	2.36

[a] The complete table is provided with the supporting information. [b] Symmetry-independent values are recorded.

$[Ti_{14}C_{13}]^+$. Other possible structures for Ti_8C_{13} have not been calculated here.

Photodissociation of $Ti_{14}C_{13}$. I have modeled the sequence of extrusions of Ti from $Ti_{14}C_{13}$ by optimizing the structures of the first three intermediates, $Ti_{13}C_{13}$, $Ti_{12}C_{13}$, and $Ti_{11}C_{13}$. The general pathway follows the suggestion of Pilgrim and Duncan,[17a] with sequential loss of the face-centering Ti atoms of $Ti_{14}C_{13}$. From the pattern that develops, the last three stages of the sequence and the structures of $Ti_{10}C_{13}$ and Ti_9C_{13} become obvious. The complete sequence involves a large degree of concerted atom rearrangement and bond breaking and making.

$Ti_{13}C_{13}$. The starting point for optimization of the first intermediate, $Ti_{13}C_{13}$, was generated by removal of Ti9 from **14/13** and movement of the two adjacent C atoms in the directions shown in diagram **14/13** (Figure 1) to a separation of 2.05 Å. No other atoms of **14/13** were moved. On optimization in symmetry C_{2v} there was substantial rearrangement, principally of these two C atoms and the four surrounding Ti atoms, to generate a structure with a C_2 group (C−C 1.33 Å) parallel to the edges of rectangular Ti1, Ti2, Ti3, Ti4. However this conformation of the incipient C_2 group constrained to be parallel to the edges of the Ti_4 quadrilateral is well-known from the Ti_8C_{12} geometry−energy surface to be less stable than the conformation in which C_2 is diagonal to the Ti_4 quadrilateral. Therefore optimization was continued without this constraint, starting with a small twist of the C_2 group and retaining only C_2 symmetry. The resulting optimized structure is presented in Figure 1 as **13/13**, occurring for both $[Ti_{13}C_{13}]$ and $[Ti_{13}C_{13}]^+$. The favorability of the diagonal conformation in symmetry C_2 is shown (see Table 1) by the improvement in binding energy by 22 kcal mol^{-1} for $[Ti_{13}C_{13}]^0$ and by 20 kcal mol^{-1} for $[Ti_{13}C_{13}]^+$.

The following atom-labeling conventions are followed for **13/13** and subsequent optimized intermediates: Ti atoms retain their numbers in structure **14/13**; single C atoms are labeled C*xy* where *x* and *y* are the lowest numbers for the Ti atoms to which C*xy* is bound; C atoms in C_2 groups are labeled C*xyz*, where Ti*x*, and Ti*y* are the side-bound Ti atoms and Ti*z* is bonded to the end of the C_2 group.

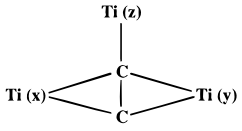

Table 4 contains selected dimensions of **13/13**, with explicit assignment of the antecedents of each bond in structure **14/13**.[57] Again the computed dimensions are not significantly dependent on the overall charge. The primary geometrical change is the contraction of the Ti_4 rhombus Ti1, Ti2, Ti3, and Ti4 around the extruded Ti and the complete formation of new C_2 group with C−C = 1.36 Å along a diagonal of the Ti_4 rhombus. A series of secondary metrical changes are significant for the Ti extrusion mechanism: (1) the Ti−C bond lengths for the lateral and longitudinal coordination of the C_2 group are virtually the same as those in the final structure Ti_8C_{13}; (2) the C^c-Ti^3 (i.e. to Ti1, Ti3) which will become C^c-Ti^i in Ti_8C_{13} are shortened by 0.5 Å relative to those (to Ti2, Ti4) destined to become C^c-Ti^o in Ti_8C_{13}, and by 0.75 Å relative to C^c-Ti^3 in $Ti_{14}C_{13}$; (3) the C^4 atoms (C12 and C34) flanking the newly formed C_2Ti_4 face are moved away; (4) relative to **14/13**, the contiguous Ti^5 atoms Ti10 and Ti13 move further from the central C atom, while the other two adjacent Ti^5 atoms, Ti11 and Ti14, move slightly closer to C^c. This movement of Ti10 and Ti13 (equivalent in C_2 symmetry) is the beginning of the extrusion of a second Ti atom.

$[Ti_{13}C_{13}]^0$ has a singly degenerate HOMO at −3.15 eV and a gap of 0.23 eV to the LUMO. The ionization energy of $[Ti_{13}C_{13}]^0$ is calculated (with lyp/b88e) to be 4.84 eV.

These calculations have simulated the final stages of the first extrusion of Ti from $Ti_{14}C_{13}$ to $Ti_{13}C_{13}$, and they substantiate the essence of the hypothesis by Pilgrim and Duncan. Further, the rearrangements of this first stage intimate the early stages of the next Ti extrusion process.

$Ti_{12}C_{13}$. In **13/13** the four antecedent Ti^5 atoms contiguous with the face which loses the first Ti atom are differentiated by the C_2 group which is formed. Two of the Ti^5 atoms (Ti10, Ti13) are further from C^c, and one of them (they are equivalent in **13/13**) will be the next to separate from the cluster. The subsequent optimization of $Ti_{12}C_{13}$ began with a structure in which Ti10 was removed, C56 and C12 were moved to within 1.4 Å of each other in parallel conformation above the irregular face formed by Ti1, Ti2, Ti5, and Ti6, and C16 and C25 were moved slightly away from the incipient C_2 group. No other atoms were moved. At this stage no symmetry remains, and further optimization was free of any constraints.

The resulting structure is **12/13**. The second C_2 group (atoms C152 and C156) twists to adopt the expected diagonal configuration across the quadrilateral of Ti1, Ti2, Ti5, and Ti6, which has changed shape from **13/13**. At the same time substantial changes are beginning to appear in other parts of the cluster, particularly around the central C atom. Selected bond distances and their antecedents are detailed in Table 5. The whole cluster is now quite dissymmetric. The original six equal C^c-Ti^5 distances have reduced to two at ca. 2.1 and two at ca. 2.6 Å. The eight equal nonbonding distances of 3.5 Å between C^c and the original Ti^3 in $Ti_{14}C_{13}$ have now become 2.1, 2.4, 2.4, 3.5, 3.6, 3.7, 3.7, and 3.8 Å. Two of the connections which will become Ti^i-Ti^o in Ti_8C_{13}, namely Ti3−Ti4 and Ti5−Ti6, are short and long, respectively. The central C atom engages three bonds at ca. 2.1 Å, and a longer connection to Ti3 at 2.44 Å, in an irregular stereochemistry.

It is evident that this represents the least symmetrical stage in the complete transformation from highly symmetrical $Ti_{14}C_{13}$ to highly symmetrical Ti_8C_{13}. It is also possible that there may be other wells on the geometry−energy surface for $Ti_{12}C_{13}$, but systematic exploration for these has not been undertaken.

$Ti_{11}C_{13}$. In structure **12/13** four of the original Ti^5 atoms remain, but as is apparent from Figure 1 and Table 5, two of these (Ti11 and Ti14) have moved well away from the central C atom, and the next stage of extrusion involves one of them. The progression to $Ti_{11}C_{13}$ involved removal of Ti11 and approach of C16 and C47 to a separation of 1.4 Å, parallel to

Table 5. Selected Interatomic Distances (Å) for the Optimized Structure, **12/13**, of $[Ti_{12}C_{13}]^0$, Symmetry C_1

bond antecedent in $Ti_{14}C_{13}$	interaction in subsequent structures (in Ti_8C_{13})	bond in $Ti_{12}C_{13}$	$[Ti_{12}C_{13}]^0$
C^6-Ti^5	–	C^c-Ti13	2.09
C^6-Ti^5	–	C^c-Ti12	2.14
C^6-Ti^5	–	C^c-Ti14	2.60
C^6-Ti^5	–	C^c-Ti11	2.59
C^6-Ti^3	C^c-Ti^i	C^c-Ti1	2.10
C^6-Ti^3	C^c-Ti^i	C^c-Ti3	2.43
C^6-Ti^3	C^c-Ti^i	C^c-Ti5	3.81
C^6-Ti^3	C^c-Ti^i	C^c-Ti7	3.54
C^6-Ti^3	C^c-Ti^o	C^c-Ti4	2.37
C^6-Ti^3	C^c-Ti^o	C^c-Ti2	3.71
C^6-Ti^3	C^c-Ti^o	C^c-Ti6	3.70
C^6-Ti^3	C^c-Ti^o	C^c-Ti8	3.64
Ti^3-C^4	Ti^i-C	Ti1−C132	2.36
Ti^3-C^4	Ti^i-C	Ti1−C134	2.34
Ti^3-C^4	Ti^i-C	Ti3−C132	2.39
Ti^3-C^4	Ti^i-C	Ti3−C134	2.20
Ti^3-C^4	Ti^o-C	Ti2−C132	2.12
Ti^3-C^4	Ti^o-C	Ti4−C134	2.17
Ti^3-C^4	Ti^i-C	Ti1−C152	2.21
Ti^3-C^4	Ti^i-C	Ti1−C156	2.24
Ti^3-C^4	Ti^i-C	Ti5−C152	2.15
Ti^3-C^4	Ti^i-C	Ti5−C156	2.36
Ti^3-C^4	Ti^o-C	Ti2−C152	2.01
Ti^3-C^4	Ti^o-C	Ti6−C156	2.02
	Ti^i-Ti^o	Ti1−Ti2	2.88
	Ti^i-Ti^o	Ti3−Ti4	2.69
	Ti^i-Ti^o	Ti1−Ti4	3.22
	Ti^i-Ti^o	Ti2−Ti3	3.64
	Ti^i-Ti^o	Ti1−Ti6	2.87
	Ti^i-Ti^o	Ti2−Ti5	2.94
	Ti^i-Ti^o	Ti5−Ti6	4.09
	Ti^i-Ti^i	Ti1−Ti3	3.54
	Ti^i-Ti^i	Ti1−Ti5	3.66
	C−C	C132−C134	1.34
	C−C	C152−C156	1.38

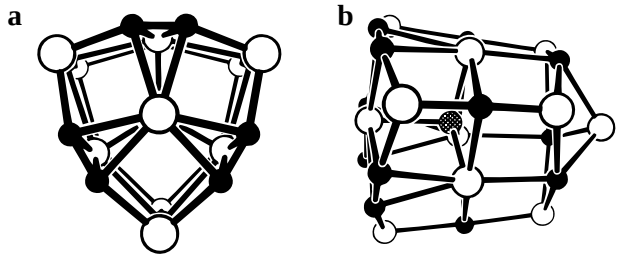

Figure 2. (a) Threefold view of structure **11/13**. (b) Side view of **11/13**.

the edges of the Ti1, Ti4, Ti7, and Ti6 quadrilateral. The geometry optimization from this point, again without any imposed symmetry, involved large rearrangements of the whole cluster, resulting in structure **11/13** with three C_2 groups.

The striking result is that the 3-fold symmetry present originally in $Ti_{14}C_{13}$ but totally removed by the first and second extrusions is recovered in $Ti_{11}C_{13}$. Figure 2a demonstrates the 3-fold symmetry of **11/13**, and the surface feature (the "wheel") characteristic of Ti_8C_{12} and Ti_8C_{13} in which a Ti^i atom is surrounded by three laterally bonded C_2 groups and three Ti^o atoms. Figure 2b is a view of **11/13** almost perpendicular to the virtual 3-fold axis, showing the $Ti_4(C_2)_3$ wheel at the reconstructed end, and the vestiges of the cubic **14/13** structure at the other. **11/13** is the hybrid intermediate structure in the transformation of **14/13** to **8/13**. The central carbon atom is now clearly coordinated in approximate tetrahedral geometry to only the four Ti atoms (Ti1, Ti3, Ti5, Ti7), which are to become the Ti^i atoms of **8/13**: the tetrahedral $C^c(Ti^i)_4$ coordination is trigonally compressed toward trigonal pyramidal, with $Ti^i-C^c-Ti^i$ angles of 101, 117°.

Attention should be drawn to some of the substantial changes between **13/13**, **12/13**, and **11/13**. Atoms such as C25 started as C^4 in **14/13**, experienced minor perturbation in **13/13**, but by **12/13** had become three-coordinate C^3, and then in **11/13** becomes C^4 but bonded to a different set of Ti atoms: C25 moves from one orthogonal 4-fold coordination to a different 4-fold orthogonal coordination, and by structure **11/13** the same has happened to C34 and C67.

A summary of selected geometrical details for the optimized structure, **11/13**, of $[Ti_{11}C_{13}]^0$ and $[Ti_{11}C_{13}]^+$ is presented in Table 6,[57] in the context of the bond antecedents in $Ti_{14}C_{13}$ and the eventual bonds of Ti_8C_{13}. There are no major geometrical differences between optimized $[Ti_{11}C_{13}]^0$ and $[Ti_{11}C_{13}]^+$. From Table 6 it can be seen that in the positive ion C−C is marginally shorter, the Ti^i-Ti^o distances are marginally longer but the Ti^i-Ti^i distances are the same, and the Ti^i-C distances around Ti1 are the same but Ti^o-C distances are marginally longer.

Optimized $[Ti_{11}C_{13}]^0$ is characterized (lyp/b88e calculation) by a HOMO-LUMO separation of 0.67 eV. The partial charges for $[Ti_{11}C_{13}]^0$ are the following: C^c −0.77; Ti1 +0.75; Ti2 +0.67; Ti4 +0.67; Ti6 +0.66; Ti3 +0.80; Ti5 +0.82; Ti7 +0.80; Ti12, Ti13, Ti14 +0.68; Ti8 +0.65; C132, C134, C152, C156, C174, C176 −0.41 to −0.43; C25, C34, C67 −0.74; C38, C58, C78 −0.77.

Intermediates $Ti_{10}C_{13}$ and Ti_9C_{13}. The structural progress of the conversion of $Ti_{14}C_{13}$ to $Ti_{11}C_{13}$ reveals all of the principles and geometrical details which will occur during the subsequent extrusion of the fourth and fifth titanium atoms, and the structure of Ti_8C_{13} after extrusion of the sixth has already been described. The probable structures and dimensions of the two remaining intermediates $Ti_{10}C_{13}$ and Ti_9C_{13} are readily predicted, and are shown as **10/13** and **9/13** in Figure 3. These intermediates were not optimized.

Energy Changes. The favorability of the structural rearrangements is reflected in the binding energies of the optimized structures of $Ti_{14}C_{13}$, the intermediates, and Ti_8C_{13} (see Table 7). In order to compare clusters with different compositions, the binding energies (BE) have been normalized, in two ways. Division of the BE by the number of atoms provides an indication of the relative BE and of changes in BE during the course of the extrusion sequence and allows comparison with the BE for solid TiC. However, the ratio of light and heavy atoms is changing during this sequence, and so normalization by atom count introduces a bias. Therefore the binding energies have also been normalized according to total number of electrons, BE/$\sum Z$. Although this quantity has no absolute significance, its change is a better indicator of the change in BE during the sequence of reactions. All of these quantities are presented in Table 7. The incremental binding energies per atom (ΔBE) relative to $Ti_{14}C_{13}$ are plotted in Figure 4, together with the binding energies per electron for both the neutral and positive clusters.

Independently of whether the cluster is calculated as positive ion or neutral molecule, the BE per atom increases from $Ti_{14}C_{13}$ to $Ti_{13}C_{13}$, changes little to $Ti_{12}C_{13}$, followed by a sharp decrease to $Ti_{11}C_{13}$, and a further decrease to Ti_8C_{13}. It is noted that the energy changes reported this way are small, $<\pm 6$ kcal mol^{-1} atom^{-1}. The normalization by number of electrons avoids the bias in the preceding analysis due to the fact that the products are becoming richer in the smaller atom carbon. The values of BE/$\sum Z$ (Figure 4b) are hardly changed in the first two stages, and then become increasingly negative throughout the sequence. The extrusion energies, that is $\{E[Ti_{n-1}C_{13}]^+ + E(Ti^0) - E[Ti_nC_{13}]^+\}$, are +274, +158, and +30 kcal mol^{-1} for the first three stages, respectively (n = 14, 13, 12; $E(Ti^0)$ = +16 kcal

Table 6. Selected Interatomic Distances (Å) and Angles (deg) for the Optimized Structure, **11/13**, of $[Ti_{11}C_{13}]$ and $[Ti_{11}C_{13}]^+$ [a]

bond antecedent	bond type in Ti_8C_{13}	bond type in $Ti_{11}C_{13}$	$[Ti_{11}C_{13}]^0$ lyp/b88e	$[Ti_{11}C_{13}]^+$ vwn/b88e
C^c-Ti^5		C^c-Ti12, Ti13, Ti14	3.34	3.35, 3.36
	C^c-Ti^i	C^c-Ti1	2.02	2.02
	C^c-Ti^i	C^c-Ti3, Ti5, Ti7	1.90	1.89
	C^c-Ti^o	C^c-Ti2, Ti4, Ti6	3.24	3.27, 3.28
	C^c-Ti^o	C^c-Ti8	3.74	3.71
	Ti^i-Ti^o	Ti1−Ti2, Ti4, Ti6	2.95	2.99, 3.00
	Ti^i-Ti^o	Ti3, Ti5, Ti7−Ti2, Ti4, Ti6	3.07−3.15	3.11−3.19
	Ti^i-Ti^i	Ti1−Ti3, Ti5, Ti7	3.00	3.02, 3.03
	Ti^i-Ti^i	Ti3, Ti5−Ti5, Ti7	3.23, 3.24	3.21, 3.22
	C−C	C132−C134 C152−C156 C174−C176	1.36, 1.37	1.34
	Ti^i-C	Ti1−C (C_2)	2.25−2.27	2.26, 2.27
	Ti^i-C	Ti3, Ti5, Ti7−C (C_2)	2.32−2.35	2.35−2.38
	Ti^o-C	Ti2, Ti4, Ti6−C (C_2)	2.00, 2.01	2.04, 2.05
Ti^3-C^4		Ti2,Ti4,Ti6−C	1.98	1.97
Ti^5-C^4		Ti12,Ti13,Ti14−C	1.92	1.93
Ti^3-C^4		Ti3, Ti5, Ti7−C25, C34, C67	2.36−2.39	2.35−2.40
Ti^3-C^4		Ti3, Ti5, Ti7−C38, C58, C78	2.26, 2.27	2.21−2.23
Ti^3-C^4		Ti8−C38, C58, C78	2.04, 2.05	2.05
Ti^5-C^4		Ti12, Ti13, Ti14−C38, C58, C78	2.08, 2.09	2.09−2.12
	$Ti^i-C^c-Ti^i$	Ti1−C^c−Ti3, Ti5, Ti7	100	101
	$Ti^i-C^c-Ti^i$	Ti3,Ti5−C^c−Ti5, Ti7	117	116, 117

[a] There is virtual C_{3v} symmetry, and values equivalent in C_{3v} are combined.

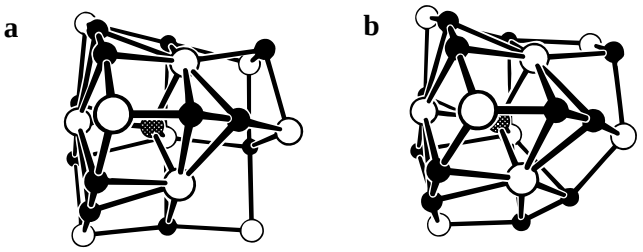

Figure 3. (a) Side view of postulated **10/13**, with the new C_2 group at the front. (b) Side view of postulated **9/13**.

mol^{-1}). The aggregate of the extrusion energies for the last three stages is +365 kcal mol^{-1}.

The general conclusions from these calculations of the binding energies are the following: (1) the first stage of the disruption of $Ti_{14}C_{13}$ through photoextrusion of Ti is the most unfavorable thermodynamically; (2) the second stage is more favorable; (3) the intermediate $[Ti_{11}C_{13}]^+$ with 3-fold symmetry and with structural features of $[Ti_8C_{13}]^+$ in place is energetically favorable; (4) the thermodynamic energy requirements for the fourth, fifth, and sixth extrusions of Ti atoms are less than those of the first three. Note that the energy barriers for the extrusion and rearrangement reactions have not been calculated.

Discussion

The occurrence of $Ti_{14}C_{13}$ as a face-centered cubic fragment of the TiC lattice is reinforced in these non-local density functional calculations. It is significant that the optimum Ti−Ti distance in many $[Ti_xC_y]^+$ clusters, 2.8−3.0 Å, is $\sqrt{2}$ times the optimum Ti−C distances of 1.9−2.1 Å, supporting the geometrical advantage of a cubic lattice. No alternative connectivity has been proposed for the $Ti_{14}C_{13}$ cluster. The DF calculations show the magnitude (ca. 0.13 Å) of the expected contraction of the vertex Ti^3 atoms into the $Ti_{14}C_{13}$ cluster, because the Ti^3 are undercoordinated. The Ti^3 atoms also bear most of the increased positive charge on ionization of $Ti_{14}C_{13}$. It is predicted that $Ti_{14}C_{13}$ will undergo addition of ligands at these vertex sites.

For Ti_8C_{13}, details of the geometry, energy and electronic structure are provided, with the hypothesis that there is a slight compressive strain on the central carbon atom. It is noted that the cluster framework with a tetracapped tetrahedron of metal atoms centered with a ligand atom, as occurs in Ti_8C_{13}, is known in other metal clusters such as $SCd_8(SR)_{12}X_4$,[65] where the four outer metal atoms are also terminally coordinated.

The mechanism proposed by Pilgrim and Duncan for the sequence of extrusion reactions is supported and substantiated by the optimizations of the structures of the intermediates. Even though the calculations refer only to the observed intermediates and not the transition states, the concerted geometrical changes associated with each extrusion of Ti and concomitant formation of a C−C bond are evident. The optimized structure of each intermediate is partly prepared for the next stage of the extrusion process.

During the full transformation from high-symmetry $Ti_{14}C_{13}$ (O_h) to high-symmetry Ti_8C_{13} (T_d), there is complete loss of symmetry at the intermediate $Ti_{12}C_{13}$, but recovery of symmetry (C_{3v}) in $Ti_{11}C_{13}$. At the distorted $Ti_{12}C_{13}$ intermediate there is maximum change in the bonding to the central carbon atom, which appears to direct the rearrangements of Ti atoms around it, and also coordination changes ($C^4 \rightarrow C^3 \rightarrow C^4$) for other carbon atoms. By the stage of intermediate $Ti_{11}C_{13}$ the four C^c-Ti^i bonds of the final product are in place and the stereochemistry at C^c approaches tetrahedral. $Ti_{11}C_{13}$ manifests a completely formed face with the $Ti^i(C_2)_3(Ti^o)_3$ geometry characteristic of Ti_8C_{13}. Note that the first three Ti^5 atoms to be extruded are mutually *cis* in the octahedral array of $(Ti^5)_6$ in $Ti_{14}C_{13}$.[66]

The changes in total energy are consistent with the interpretation of the changes in geometry, namely that $Ti_{13}C_{13}$ and $Ti_{12}C_{13}$ are the least stable intermediates, with considerable gain in

(65) (a) Dance, I. G. *Aust. J. Chem.* **1985**, *38*, 1391−1411. (b) Lee, G. S. H.; Fisher, K. J.; Craig, D. C.; Scudder, M. L.; Dance, I. G. *J. Am. Chem. Soc.* **1990**, *112*, 6435−7. (c) Dance, I. G.; Fisher, K. J.; Lee, G. S. H. In *Metallothioneins: synthesis, structure and properties of metallothioneins, phytochelatins and metal thiolate complexes*; Stillman, M. J., Shaw, C. F., Suzuki, K. T., Eds.; VCH Press: New York, 1992; pp 284−345. (d) Lee, G. S. H. Thesis, UNSW, 1992; (e) Dance, I. G.; Fisher, K. J. *Prog. Inorg. Chem.* **1994**, *41*, 637−803.

(66) The alternative mechanism in which vertex Ti^3 atoms are lost from $Ti_{14}C_{13}$ has been considered but rejected, because (a) the cyclic C_3 so generated has no precedent in these clusters (acyclic C_3 is feasible), (b) loss of Ti^3 does not reduce the high coordination of C^6, (c) a mechanism with concerted minor rearrangements is not apparent, and (d) there are eight Ti^3 but only six Ti atoms to be lost.

Table 7. Binding Energies (BE, kcal mol^{-1} for the Optimized Clusters $Ti_{14}C_{13}$, $Ti_{13}C_{13}$, $Ti_{12}C_{13}$, $Ti_{11}C_{13}$, and Ti_8C_{13} as Neutral Clusters and Positive Ions

	charge 0	charge +	charge 0			charge +		
structure	BE lyp/b88e	BE vwn/b88e	BE per atom[a]	ΔBE per atom	BE/$\sum Z$ BE per electron[b]	BE per atom[a]	ΔBE per atom	BE/$\sum Z$ BE per electron[b]
14/13	−3716	−3449	−137.6	0	−9.63	−127.7	0	−8.93
13/13	−3468	−3191	−133.4	+4.2	−9.53	−122.7	+5.0	−8.77
12/13	−3347	−3049	−133.9	+3.7	−9.79	−122.0	+5.7	−8.91
11/13	−3329	−3035	−138.7	−1.1	−10.40	−126.4	+0.7	−9.48
8/13	−2980	−2718	−141.9	−4.3	−11.73	−129.4	−1.7	−10.70

[a] BE normalized by the number of atoms in the cluster. [b] BE normalized by the number of electrons in the cluster: see text.

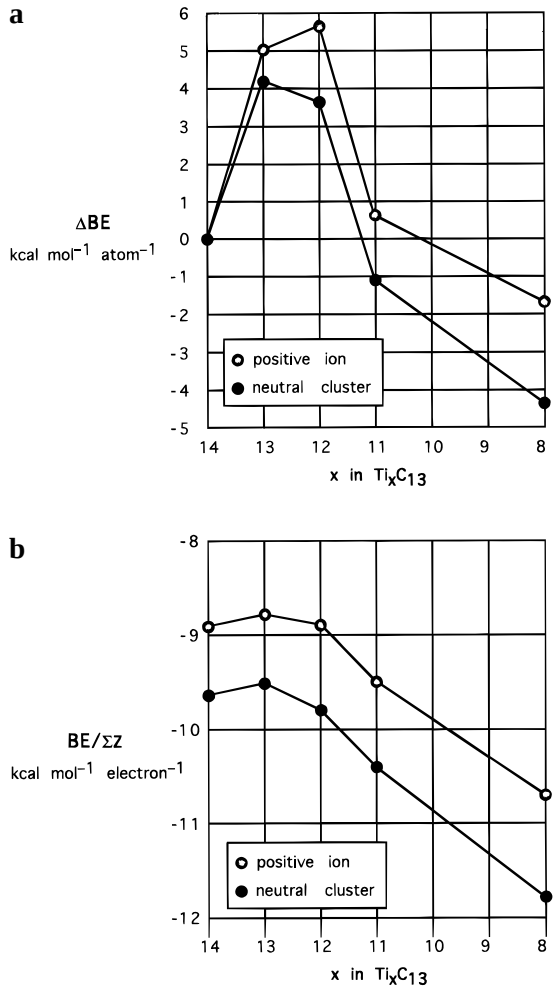

Figure 4. Comparative binding energies for the reactant, intermediate, and product clusters in the dissociative sequence: closed circles are neutral clusters (lyp/b88e), open circles are positive ions (vwn/b88e). (a) Incremental binding energies, ΔBE, per atom, in kcal mol^{-1} atom^{-1}. (b) Binding energies (kcal mol^{-1}) per electron, BE/$\sum Z$, in the clusters.

stability in the stage $Ti_{12}C_{13} \rightarrow Ti_{11}C_{13}$. Thereafter the reaction appears to cascade to Ti_8C_{13}, with parallel improvements in energy and geometry. Pilgrim and Duncan discussed the energy changes involved in these photodissociations and considered that the photon energy supplemented enhanced internal energy in effecting the dissociations. Concomitant with the changes in geometry and energy, there is improvement in the electronic structure. The TiC fragment $Ti_{14}C_{13}$ is characterized by closely spaced partially occupied orbitals at the Fermi level. The HOMO-LUMO gap of 0.2 eV in $Ti_{14}C_{13}$ is maintained through $Ti_{13}C_{13}$ and $Ti_{12}C_{13}$, but increases to 0.67 eV in $Ti_{11}C_{13}$ and to 1.0 eV in Ti_8C_{13}.

The computed binding energies are considered to be reliable. Data for direct assessment against experiment are not available, but calibration can be made via the the cohesive energy of solid TiC, 7.1 eV mol^{-1}.[32b] The computed binding energy for $Ti_{14}C_{13}$ using gradient corrections to the density functionals is 15% less than the cohesive energy of TiC, which is consistent with the decreased stabilization of the surface atoms of a molecular cluster relative to the totally non-molecular solid.

The calculations of geometry and energy for $Ti_{13}C_{13}$ have confirmed the stability of the configuration in which the C_2 group is aligned over the long diagonal of a Ti_4 rhombus. This is the configuration which contributes to the stability of the T_d isomer of Ti_8C_{12} over the T_h isomer. The stabilization of this C_2M_4 configuration relative to the alternative in which C_2 is parallel to the edges of reactangular M_4 is the crucial factor in the model for the binding and activation of N_2 to the Fe_4 face of the Fe_7S_9Mo cluster at the active site of nitrogenase:[67] the bound N_2 is isoelectronic with C_2^{2-} of metallocarbohedrenes. The results for $Ti_{13}C_{13}$ reported here provide insight into the energy advantage of the diagonal-rhombus configuration, because the two different C_2Ti_4 configurations (in the optimized structures with symmetry C_2 and C_{2v}) are not associated with other substantial changes in the cluster core. The energy advantage of the diagonal-rhombus configuration is 21 kcal mol^{-1}. This value can be used to delve into the energy contributions of the stability of T_d-Ti_8C_{12} over T_h-Ti_8C_{12}.[42]

The reaction analyzed here is the formation of C−C bonds in the presence only of metal atoms. This is a fundamental process, which relates to the catalysis of carbon coupling at metal surfaces, to the formation of networked metallofullerenes, and to the metal-catalyzed growth of nanotubes. Other photodissociations of metal atoms from metallocarbohedrenes described by Pilgrim and Duncan[17] involve further loss of metal and clusters with higher C/M ratios and the formation of larger carbon networks. Modeling of these structures and processes using non-local density functional theory is in progress.

Acknowledgment. This research is funded by the Australian Research Council. I gratefully acknowledge provision of computing resources by Australian Numerical Simulation and Modelling Services, and by the Australian Nuclear Science and Technology Organisation and the University of NSW.

Supporting Information Available: Details of the basis sets and tabulations of all dimensions and atomic coordinates, including a complete Table 4 (10 pages). This material is contained in libraries on microfiche, immediately follows this article in the microfilm version of the journal, can be ordered from the ACS, and can be downloaded from the Internet; see any current masthead page for ordering information and Internet access instructions.

JA9529089

(67) Dance, I. G. *Aust. J. Chem.* **1994**, *47*, 979−990.